



The performance of phosphoric acid in the preparation of activated carbon-containing phosphorus species from rice husk residue

Yiping Luo¹ , Dong Li^{1,*} , Yichao Chen¹ , Xiaoying Sun¹ , Qin Cao¹ ,
and Xiaofeng Liu^{1,*}

¹ Key Laboratory of Environmental and Applied Microbiology, Environmental Microbiology Key Laboratory of Sichuan Province, Chengdu Institute of Biology, Chinese Academy of Sciences, No. 9, Section 4, Renmin Nan Road, Chengdu 610041, Sichuan, People's Republic of China

Received: 11 October 2018

Accepted: 30 November 2018

Published online:

6 December 2018

© Springer Science+Business Media, LLC, part of Springer Nature 2018

ABSTRACT

The performance of phosphoric acid (H_3PO_4) in the preparation of activated carbon-containing phosphorus species (P-species) using rice husk residues as feedstock was studied. In the activation process, the consequent pretreatments by NaOH and HCl, respectively, remove the silica and ash thoroughly, which led to cracks and pore opening. While H_3PO_4 acting as activation reagent interacted with the phenolic and carbonyl groups of activated carbon, forming P-containing carbonaceous species (such as C–O–P), which further promoted the development of micropore of the activated carbon and then increased the surface area, H_3PO_4 also acted as catalyst to adjust and control the texture properties and structures of activated carbon. The activated carbon (PC-2.5) prepared at 500 °C for 2 h using H_3PO_4 -treated carbon residue with acid/carbon mass ratio of 2.5 (g/g) achieved the maximum surface area of 1365 m²/g. Interestingly, the P-species formed in the activated carbon exhibited high-efficiency catalytic effects for the treatment of municipal waste landfill leachate to a disposable quality, where the removal rate of pollutant from landfill leachate over 90% and a high removal of TN (84%), COD (82%) and NH_4^+ -N (100%) were obtained.

Introduction

Because of the over-dependence of petroleum-based resources and the increase in global environmental problems, biomass was viewed as a sustainable

feedstock to produce bio-oil and syngas for the replacement of the limited fossil resources [1, 2]. However, a large amount of waste residues were generated in the process, which were commonly used as low-value energy resource, burned in the field or discarded [3, 4]. An economic approach was the

Address correspondence to E-mail: lidong@cib.ac.cn; liuxf@cib.ac.cn

utilization of these waste residues with high carbon content to produce useful materials, which had good economical and environmental prospects.

Activated carbon was a useful carbonaceous material with high surface area and controllable pore structure, which was generally used as adsorbent for the removal of a wide variety of organic and inorganic pollutants from wastewater in industry [5, 6]. The preparation of high-performance activated carbon from these agricultural waste residues was promising for the development of low-cost and sustainable bio-refinery.

The preparation of activated carbon from biomass residues generally involved physical and chemical method (Table 1) [4, 7, 8]. Fu et al. [9] have summarized the characteristics of the two different activation methods. The main difference between the two processes was the activating agent and carbonization temperature. The physical activation needed a very

high temperature (> 900 °C) in the presence of steam or CO₂ [9]. Compared with physical activation method, chemical activation could be carried out at relatively lower temperature and hence reduces energy consumption [10]. In addition, activated carbon produced from chemical activation was reported to have higher surface area as well as well-developed porosity compared with that produced from physical activation [11]. In recent researches, the chemical activation agents mostly used included ZnCl₂ [12–14], strong base (NaOH or KOH) [9, 15–18] and H₃PO₄ [14, 17]. Among these activation agents, H₃PO₄ has received wide attention because of its easy recovery and minimal environmental impacts [17]. The H₃PO₄-activated carbon has been used in the removal of dyes, heavy metal ions from both modeled aqueous solutions [13, 19–22] and real wastewater [23, 24]. The preparation of high-performance activated carbon in this process was significantly

Table 1 Literature comparison of activated carbons from biomass

Activation method	Conditions	S _{BET} (m ² /g)	Applications	References
Physical activation of rice husk	Ferric nitrate, N ₂ , 750 °C, 1.5 h	527	Phenol hydroxylation	Zhang et al. [7]
Physical activation of rice husk	Stem, 800 °C, 15 min	1365	–	Alvarez et al. [8]
Physical activation of rice husk	CO ₂ , 800 °C, 45 min	1514	–	Alvarez et al. [8]
Chemical activation of Douglas fir pellets	81.21% H ₃ PO ₄ , N ₂ , microwave-assisted pyrolysis, 450 °C, 48 min	1725.7	–	Villota et al. [4]
Chemical activation of rice husk	H ₃ PO ₄ , N ₂ , 500 °C, 1 h	1016	–	Li et al. [17]
Chemical activation of rice husk	First step: N ₂ , 450 °C, 3 h Second step: KOH, N ₂ , 750 °C, 1 h	2138	Phenol adsorption	Fu et al. [9]
Chemical activation of corn stalks	First step: 550 °C, 1.5 h, N ₂ Second step: KOH, 550 °C, 1.5 h, N ₂	677	Sorbent of Cd ²⁺ from water	Zubrik et al. [11]
Chemical activation of rice husk	NaOH, 800 °C, 2 h, N ₂	2841	Phenol adsorption	Song et al. [15]
Chemical activation of sugarcane bagasse	KOH, 687 °C, 2 h, N ₂	99.94	Landfill leachate treatment	Azmi et al. [16]
Chemical activation of rice husk	KOH, 750 °C, 2 h, N ₂	1773	–	Fu et al. [18]
Chemical activation of coconut shells	Hydrothermal pretreatment, ZnCl ₂ , 850 °C, 2 h, N ₂	1744	Adsorption of textile dyes	Jain et al. [12]
Chemical activation of olive stone	ZnCl ₂ , 850 °C, 2 h, N ₂	790.25	Removing Cd(II)	Kula et al. [13]
Chemical activation of coffee grounds	ZnCl ₂ + H ₃ PO ₄ , 600 °C, 45 min, N ₂	640	Adsorption of phenols and acid and basic dyes	Namane et al. [14]

important. Therefore, the investigation for the formation mechanism of activated carbon structure in the activation process presented unique challenges and opportunities. Li et al. [17] proposed that H_3PO_4 might incorporate into carbon through C–O–P bonds acting as a reagent in the activation process. Puziy et al. [25] reported that phosphate-like structure bound carbon lattice via C–O–P bonding was formed in H_3PO_4 activation process. What was the role of H_3PO_4 in the activation process and how the structure of activated carbon formed needed further investigation, which could give valuable ideas for the preparation of high-performance carbon materials.

The treatment of landfill leachate as heavily polluted water was the prerequisite to meet the discharge standards without environment effects [26]. Herein, we achieved the preparation of high-performance activated carbon by H_3PO_4 activation using rice husk residue, and the prepared activated carbon-containing P-species exhibited great application prospect in the treatment of landfill leachate. The investigation focuses on the performance of H_3PO_4 in the preparation of activated carbon-containing phosphorus species (P-species). One possible porous structure formation mechanism of activated carbon-containing P-species by H_3PO_4 activation was proposed, which provided useful information for the preparation of high-performance carbon materials using agricultural waste residues by adjusting and controlling the texture properties and structures of activated carbon.

Materials and methods

Materials

Rice husk residue (obtained from Chongqing Jinhuan Biomass Energy Company) was produced in a fluidized bed reactor, where rice husk was heated to 400 °C to produce bio-oil for the replacement of limited fossil resources. Sodium hydroxide (NaOH, AR, Chengdu Kelong Chemical Reagent Factory in China), hydrochloric acid (HCl, 36–38%, Chengdu Kelong Chemical Reagent Factory in China) and phosphoric acid (H_3PO_4 , 85%, Chengdu Jinshan Chemical Reagent Factory in China) were purchased commercially and used without further purification. Landfill leachate collected from municipal solid waste landfill site in Luodai, Chengdu, was filtrated

by sodium membrane and diluted by 12.5 times with water before use.

Pretreatment of the obtained rice husk residue

Rice husk residue (20–40 mesh, abbreviated as OC) was washed with deionized water to remove floating carbon and impurities and then dried at 105 °C in an oven overnight. After that, OC was consecutively treated by 3 mol/L NaOH and 6 mol/L HCl. In a typical run, 30 g of dried OC with 200 mL 3 mol/L NaOH was added in a 500-mL round-bottom flask firstly and then heated to 105 °C for 5 h to remove silica. After reaction, the suspension was filtrated to obtain soluble Na_2SiO_3 formed by the reaction of NaOH with silica in rice husk residue, and base-treated solid samples were also obtained. SiO_2 can be collected from soluble Na_2SiO_3 , which had many sustainable applications, especially in catalysis, energy and environment functional materials [27], while base-treated solid samples (abbreviated as BC) were washed with deionized water and then dried in an oven for the treatment in the next step. To remove ash and impurities thoroughly, 30 g dried BC samples were put in the same round-bottom flask, and 200 mL 6 mol/L HCl solution was added into the reactor, and then, the reactor was heated to 105 °C for 5 h. After reaction, the consecutive base–acid (abbreviated as BAC)-pretreated solid samples were separated from liquid by filtration, washed to neutrality with deionized water and dried at 105 °C in an oven for use to prepare activated carbon.

H_3PO_4 activation processes

The preparation of activated carbon from rice husk residue by H_3PO_4 activation was conducted in horizontal cylindrical furnace in N_2 atmosphere. In a typical run, 2 g BAC samples were impregnated in a solution with certain concentration of H_3PO_4 and then put in an oven at 105 °C overnight to remove excess water. The dried samples obtained above were put in the furnace for activation, where it was heated from room temperature to the desired temperature at 5 °C/min and then kept at the designed temperature for different times under N_2 flow of 60 mL/min. After activation, the furnace was cooled to room temperature naturally. The solid samples collected from furnace were washed to neutral with deionized

water and dried to obtain activated carbon (named as PC-X, X means the mass ratio of H_3PO_4 to BAC), ready for the next-step test. For comparison, OC and BC were activated by H_3PO_4 using the same method.

Treatment of landfill leachate using prepared activated carbon

The carbon samples obtained above by different treatments were used for the treatment of landfill leachate. Typically, a certain amount of solid samples (1 g) with 50 mL diluted leachate was put in a 250-mL flask, and the mixture was shaken constantly (140 rpm) at 30 °C for desired time in a shaker. After filtration using 0.45- μm filter, aqueous solution was collected for analysis.

Characterization of carbon samples

The specific surface area and pore size of the solid samples were measured by N_2 adsorption at -196 °C using a Micromeritics TriStar 3020 analyzer. The BET surface area (S_{BET}) was calculated from N_2 adsorption isotherms based on the BET equation [28]. The micropore volume (V_{mic}) and the mesopore volume (V_{mes}) were calculated using t-plot method. The average pore diameter was estimated from the surface area and pore volume [29]. Pore size distributions were calculated from nitrogen adsorption results with DFT Plus Software. Prior to N_2 adsorption measurements, the samples were degassed at 120 °C for 2 h and then heated to 300 °C for 2 h in vacuum condition until a pressure of less than 10^{-2} Pa. The elemental compositions of the samples were analyzed by elemental analyzer (Italy, CARLO ERBA 1106). The FTIR spectra of solid samples were performed on a Nicolet 6700 Fourier Transform Infrared Spectrometer. The spectra of samples were recorded from 4000 to 500 cm^{-1} in attenuated total reflectance (ATR) mode with a resolution of 4 cm^{-1} and 64 scans. SEM (Phenom Pro) was used to characterize the surface morphology of samples obtained after different treatments. The samples were gold coated prior to analysis. X-Ray diffraction (XRD, Dandong Fangyuan DX-1000) was used to characterize the crystalline structure of solid samples obtained after different treatments with monochromatic $\text{Cu } K_\alpha$ radiation ($\lambda = 1.542 \text{ \AA}$) at 40 kV and 25 mA. Thermogravimetric analysis of samples obtained from different treatments was performed on Netzsch STA

449 F5 (Germany). Typically, about 10 mg sample was placed in an alumina crucible and heated from 20 °C to 800 °C with a heating rate of 20 °C/min in air (60 mL/min). The variation of surface groups on the samples with different treatments was determined by Boehm titration [30]. XPS was performed using an Axis Ultra DLD (Kratos) spectrometer with Al- K_α X-ray radiation. The energy scale was internally calibrated by setting the C1s peak at 284.6 eV.

The analysis of treated landfill leachate

The chemical oxygen demand (COD) test of liquid samples was performed by colorimetric method using Spectrophotometer HACH Model DR/1900. Before analysis, liquid samples were digested for 2 h at 150 °C using HACH DR/200 instrument. The NH_4^+ -N content of liquid samples was determined using colorimetric method according to literature [31]. The total N content (TN) was measured using Spectrophotometer HACH Model DR/1900. Prior to analysis, liquid samples were digested for 0.5 h at 120 °C using HACH DR/200 instrument. UV-Vis spectroscopy analysis of liquid samples was performed on HITACHI U-4100 Spectrophotometer (Tokyo, Japan). The removal rate of pollutant from leachate was calculated based on the intensity of ultraviolet adsorption at 254 nm.

Results

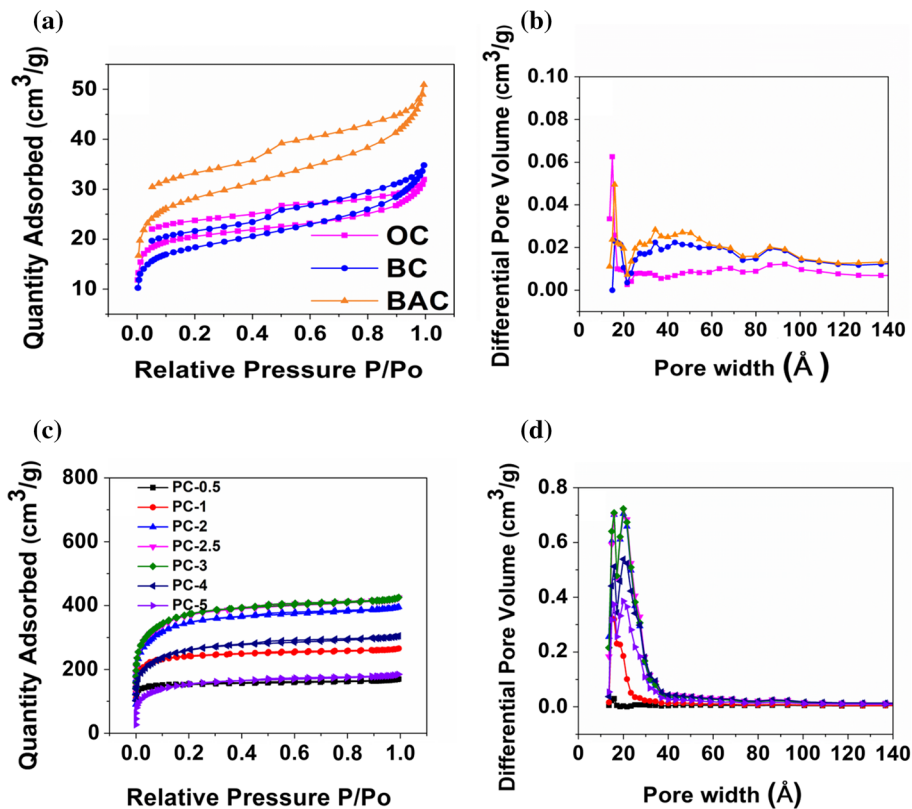
Textural properties of the carbon samples prepared with different treatments

The effect of H_3PO_4 in the activation process

The N_2 adsorption–desorption isotherms of the samples obtained with different treatments were firstly investigated. It was observed that the hysteresis loop of OC (rice husk residue) exhibited a type H4 of IUPAC classification, where the adsorption and desorption branches were parallel over the range of relative pressure tested (Fig. 1a). The hysteresis loop of type H4 was associated with specific pore structures which had slit-shaped pores or large macropores [32–34].

The similar hysteresis loop of N_2 adsorption–desorption isotherms has been observed for BC (obtained after OC was treated by NaOH) and BAC

Figure 1 Adsorption–desorption isotherms of N_2 at -196° (a, c) and pore size distributions (b, d) for samples obtained with different treatments.



(obtained after OC was consecutively treated by NaOH and HCl) samples, indicating that these porous characters remained after NaOH and HCl pretreatments. The significant increase in pore volume of N_2 adsorbed by BAC sample compared to those of OC and BC samples at higher relative pressure was observed, suggesting that there might be the presence of a substantial amount of mesopores in BAC sample [35, 36]. Moreover, as shown in Fig. 1b, the distribution of pore structure in BAC was diverse. Figure 1c shows the N_2 adsorption–desorption isotherms of activated carbon prepared at different H_3PO_4 /BAC ratios (noted as PC-X, X means the H_3PO_4 /BAC mass ratio in the treatment). These isotherms were quite different from these of OC, BC and BAC samples without H_3PO_4 activation, where the adsorption and desorption branches were closed. According to IUPAC classification, these isotherms belonged to Type I, which was characteristic of microporous materials [37]. The results suggested that H_3PO_4 activation process changed the porous structure of the samples. The pore size distribution plots of samples became concentrated after H_3PO_4 activation (Fig. 1b, d), and the pore size of samples was mainly focused on the range from 13.2 to 36.8 \AA .

Summary of textural properties of carbon samples with different treatments is presented in Table 2. It can be observed from Table 2 that the surface area, the total pore volume and microporous volume were almost unchanged after NaOH pretreatment, while these all slightly increased after consecutive NaOH and HCl pretreatment. However, the surface area increased dramatically after H_3PO_4 activation. The surface area of activated carbon prepared with H_3PO_4 /BAC ratio of 0.5 at $500^\circ C$ for 1 h reached $585\text{ m}^2/g$, which was much higher than OC ($78\text{ m}^2/g$), BC ($78\text{ m}^2/g$) and BAC ($105\text{ m}^2/g$) without H_3PO_4 activation. The surface area increased from $585\text{ m}^2/g$ with increasing H_3PO_4 /BAC ratio from 0.5 to 3 and then gradually decreased to $561\text{ m}^2/g$ with further increasing H_3PO_4 /BAC ratio to 5. It was also found that the H_3PO_4 /BAC ratio had a significant influence on the porosity of activated carbon obtained. The total pore volume and microporous volume dramatically increased after H_3PO_4 activation and showed the same trend as the surface area, with increasing H_3PO_4 /BAC ratio to 5. The inadequate development of porous structure was observed using lower H_3PO_4 concentration, which might be caused by the insufficient amount of H_3PO_4 used, and then,

Table 2 Textural properties of carbon samples with different treatments

Sample	S_{BET} (m ² /g)	V_t (cm ³ /g)	V_{mic} (cm ³ /g)	V_{mic}/V_t (%)	Pore size (Å)
OC	78	0.05	0.02	40.0	25.41
BC	68	0.05	0.02	40.0	31.58
BAC	105	0.08	0.03	37.5	30.01
PC-0.5	585	0.26	0.21	80.8	17.95
PC-1	923	0.41	0.33	80.5	17.81
PC-2	1281	0.61	0.40	65.2	19.11
PC-2.5	1365	0.66	0.43	65.2	19.27
PC-3	1379	0.67	0.44	65.7	19.09
PC-4	952	0.47	0.30	63.8	19.81
PC-5	561	0.28	0.16	57.1	20.30

the sample could not be activated effectively. However, the surface area and pore volume decreased when H₃PO₄/BAC ratio was higher than 3. Thus, higher concentration of H₃PO₄ might form some phosphorus compounds, which blocked the porosity of activated carbon. These results were in accordance with Li's work [17]. The microporous volume contributed to more than 50% of the total pore volume for activated carbon prepared with all the H₃PO₄/BAC ratios. The result suggested that H₃PO₄-activated carbon was mainly microporous material. Moreover, the average pore size of activated carbon obtained by H₃PO₄ activation ranged from 17.81 to 20.30 Å, which supported the microporosity of activated carbon prepared.

The effect of activation temperature and time in the activation process

The surface area and pore volume of activated carbon reached a maximum of 1379 m²/g and 0.67 cm³/g, respectively, at H₃PO₄/BAC ratio of 3; however, these values were only slightly higher than those obtained at H₃PO₄/BAC ratio of 2.5 (1365 m²/g and 0.66 cm³/g, respectively). Since keeping the activation process using lower H₃PO₄ concentration was more economic, the effect of activation temperature on the textural properties of activated carbon was studied at H₃PO₄/BAC ratio of 2.5 with activation time of 1 h (Figure S1 and Table S1). It could be seen that the activation temperature exhibited significant influence on the textural properties. When the sample was activated at 500 °C, it possessed the largest adsorption capacity, indicating the largest pore volume obtained under this activation condition (Figure S1). With the increase in activation temperature, the surface area of activated carbon samples

increased firstly, reached the maximum at 500 °C and then decreased (Table S1). Below 500 °C, increasing temperature was beneficial for the formation of pores in the carbon. Especially when the temperature increased from 400 to 500 °C, the surface area and pore volume increased obviously from 807 to 1365 m²/g and 0.40 to 0.60 cm³/g, respectively. However, with further increase in temperature, violent gasification reactions might cause part of the micropore structure to be destroyed by collapsing and thus led to the decrease in surface area and pore volume [34]. Therefore, the optimum activation temperature for the preparation of activated carbon was 500 °C. The variation of textural properties for activated carbons was dependent on the activation time (Figure S2 and Table S2). With activation time increased, H₃PO₄ might enhance the development of pores, so the surface area and pore volume gradually increased. After reaching the maximum value with the activation time of 1 h, the prolonging activation time led to carbon burn off and thus the structure of pore was destroyed, which decreased the surface area and pore volume. The activation time of 1 h could be considered as a suitable point.

The effect of base and acid pretreatment in the activation process

The above results implied that H₃PO₄ activation process made more porous structure. In order to study the effects of acid and base pretreatment on the textural properties of activated carbon before H₃PO₄ activation, N₂ adsorption measurement of POC-2.5, PBC-2.5 and PC-2.5 samples was taken. It can be seen from Fig. 2a that the adsorption and desorption branch of POC-2.5 remained nearly horizontal over the range of relative pressures tested, which was

characteristic of non-porous solids or large macropores [17, 30–32], indicating that only H_3PO_4 activation without consecutive NaOH and HCl pretreatment was not benefit for the development of porosity. The surface area and average pore size were, respectively, $13 \text{ m}^2/\text{g}$ and 160.26 \AA , and the pore size distributions focused on $40\text{--}140 \text{ \AA}$ mostly, which further confirmed that the pore structure was not well developed (Table 2 and Fig. 2b). The surface area and the total pore volume increased dramatically after NaOH pretreatment, especially consecutive NaOH and HCl pretreatment (Table 3). The elemental analysis results showed that the relative percentage of carbon increased in BC samples (Table S3). Because the silica was removed after NaOH pretreatment, the relative percentage of carbon increased. The pores in samples were unblocked after the removal of silica, and this promoted the development of pore structure [10]. So it could be concluded that a porous structure was developed after NaOH pretreatment. Furthermore, the significant decrease in ash was observed in BAC samples (Table S4), suggesting that HCl pretreatment to remove ash and impurities thoroughly could promote the development of porous structure. Li et al. [17] obtained a maximum surface area of $1016 \text{ m}^2/\text{g}$ for activated carbon from NaOH-treated rice husk residue using H_3PO_4 as activation agent. However, in this work the maximum surface area of activated carbon by H_3PO_4 activation could reach $1365 \text{ m}^2/\text{g}$ from consecutive NaOH–HCl-treated rice husk residue. This phenomenon further supported that consecutive base and acid pretreatment played important roles in the formation of porous structure. Additionally, we calculated the yields of activated carbon obtained after different concentrations of H_3PO_4 activation (Table S5). The formation of phosphate and polyphosphate species would increase the

mass of the obtained activated carbon, while the dehydration of H_3PO_4 and the decomposition of some functional groups occurred in this process would decrease its mass [17, 38]. With increasing concentration of H_3PO_4 , more phosphate and polyphosphate species formed, so the yield of activated carbon increased. However, part of the porosity of AC might be blocked by the formed phosphorus compounds [10]. The yield of activated carbon has no linear relationship to the surface area and pore volume. Therefore, the effect of activation temperature, activation time, the concentration of H_3PO_4 and consecutive base–acid pretreatment on the textural properties of the prepared activated carbon was studied.

Surface characteristics of carbon samples

The FTIR spectra of carbon samples obtained after different treatments are described in Fig. 3a. It was observed that the peaks at 3384 and 1703 cm^{-1} , respectively, corresponding to stretching vibration of $-\text{OH}$ (hydroxyl groups) [15] and the stretching vibration of $-\text{C}=\text{O}$ (carbonyl groups) [36], decreased and shifted after H_3PO_4 activation, which suggested that H_3PO_4 might affect $-\text{OH}$ and $-\text{C}=\text{O}$ groups. The peak at 1600 cm^{-1} corresponded to aromatic ring ($\text{C}=\text{C}$) stretching vibrations, gradually shifted to 1570 cm^{-1} with increasing H_3PO_4 concentration in the activation process. This implied that H_3PO_4 might interact with $\text{C}=\text{C}$ bonds. Puziy et al. [39] reported that the peak at $1220\text{--}1180 \text{ cm}^{-1}$ was assigned to stretching vibration of $\text{P}=\text{O}$, $\text{O}-\text{C}$ stretching vibration in $\text{C}-\text{O}-\text{P}$ linkage and $\text{P}=\text{OOH}$ bond. The peak at 1180 cm^{-1} after H_3PO_4 activation was observed (Fig. 3a), which indicated the formation of P-containing carbonaceous species in H_3PO_4 -activated

Figure 2 Adsorption–desorption isotherms of N_2 at -196° (a) and pore size distributions (b) for samples obtained after different treatments at 500°C for 1 h.

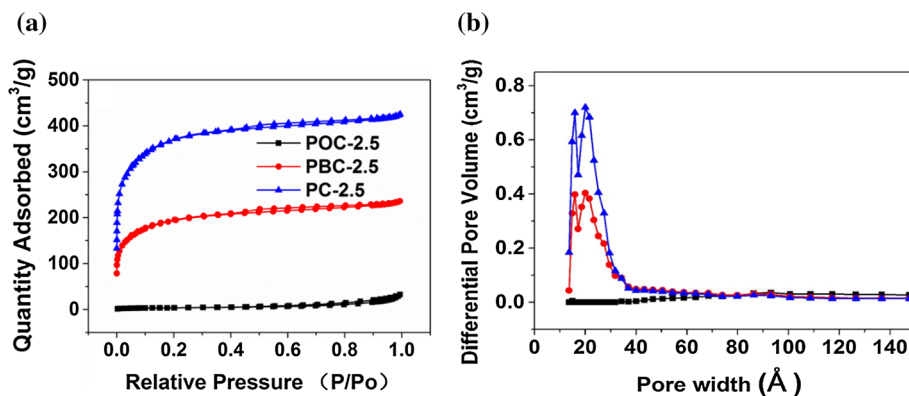
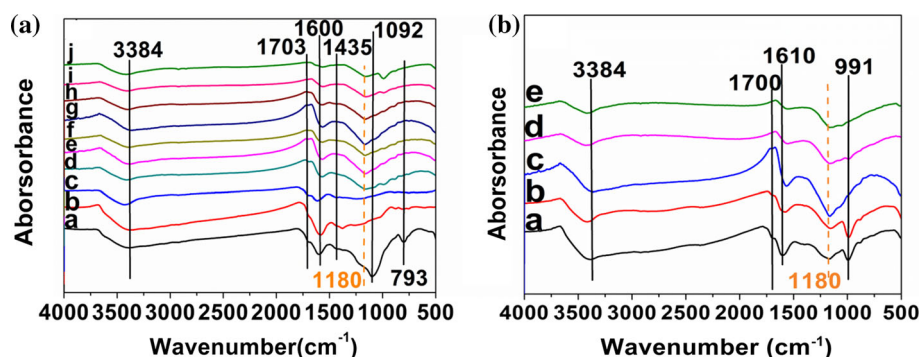


Table 3 Effect of different pretreatments on the textural properties of samples obtained at 500 °C for 1 h

Samples	S_{BET} (m ² /g)	V_t (cm ³ /g)	V_{mic} (cm ³ /g)	Pore size (Å)
POC-2.5 ^a	13	0.05	0.00	160.26
PBC-2.5 ^a	711	0.36	0.20	20.52
PC-2.5 ^a	1365	0.66	0.43	19.27

^aThe carbon samples (OC, BC and BAC) were activated by H₃PO₄; the mass ratio of acid/carbon was 2.5 in the activation process

**Figure 3** FTIR spectra of samples obtained after different treatments (a): (a) OC; (b) BC; (c) BAC; (d) PC-0.5; (e) PC-1; (f) PC-2; (g) PC-2.5; (h) PC-3; (i) PC-4; (j) PC-5 and different

activation temperatures with H₃PO₄/BAC ratio of 2.5 (b): (a) 300 °C; (b) 400 °C; (c) 500 °C; (d) 600 °C; (e) 700 °C.

carbon. There were two peaks at 1092 and 793 cm⁻¹ in OC samples, corresponding to stretching vibration of Si–O band [10]. The two peaks disappeared after NaOH pretreatment, which further supported the removal of silicon. The effect of activation temperature on the FTIR spectra of samples obtained with H₃PO₄/BAC ratio of 2.5 was also studied (Fig. 3b). The above-described peaks, such as 3384, 1700 and 1600 cm⁻¹, corresponding to the stretching vibration of –OH, –C=O and C=C bonds, all shifted with increasing activation temperature. The results suggested that activation temperature would affect the interaction of H₃PO₄ and –OH, –C=O or C=C bonds. It was worthy to note that the peak at 1180 cm⁻¹ with the highest intensity was obtained at 500 °C. Based on the above BET results, the maximum surface area of 1365 m²/g was obtained at 500 °C. It could be speculated that the P-containing carbonaceous species might be an important factor for the development of porous structure in activated carbon.

For further characterization, SEM micrographs of the samples obtained after different treatments were carried out (Fig. 4a). It could be seen that OC possessed an organized corrugated structure covering the outer epidermis of rice husk, which implied the existence of SiO₂ [13]. The surface morphology of BC samples obtained after NaOH pretreatment was

significantly varied, which exhibited some cracks and porosity in their structures. This might be due to new pores formed with the release of silica by the base pretreatment. It was observed that some pores existed in the carbon obtained after being treated by H₃PO₄ [Fig. 4a(c)–(f)]. The results supported that high surface area of activated carbon could be obtained by H₃PO₄ activation. Figure 4b shows the XRD patterns of the samples obtained from different treatments. An obvious peak appearing around at 2θ = 22.2° was the characteristic peak of silica, which corresponded to the presence of cristobalite in ash [15]. The peak corresponding to SiO₂ almost disappeared after NaOH pretreatment, while two broad peaks, respectively, appeared at approximately 2θ = 25° and 44.3°, indicating the formation of turbostratic structure of disordered carbon [40]. The two peaks were also observed after activation with H₃PO₄ but with higher intensities [Fig. 4b(c)–(g)], implying H₃PO₄ activation promoted the formation of turbostratic structure.

The TG and DTG curves of the samples obtained with different treatments in air atmosphere are shown in Fig. 4c and Figure S3. It was found that the mass loss of samples increased after being treated by NaOH, and HCl pretreatment further promoted the mass loss. Because the removal of silica and ash was

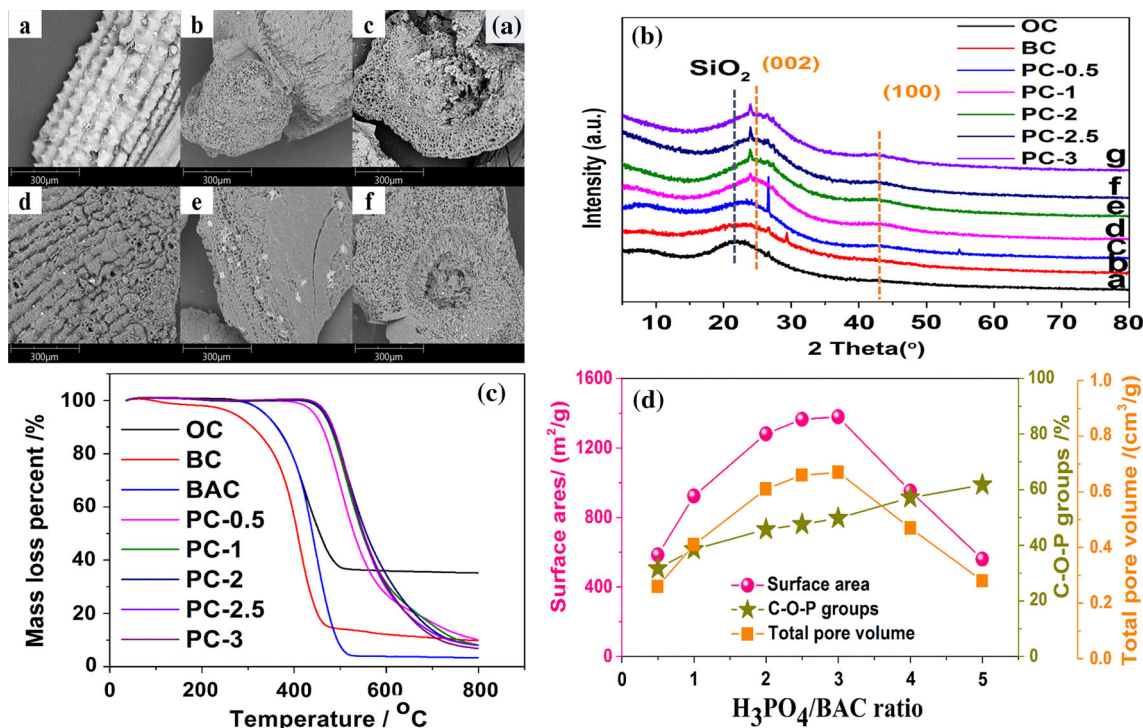


Figure 4 SEM images (a) and XRD results (b) of samples obtained after different treatments: (a) OC; (b) BC; (c) PC-0.5; (d) PC-1; (e) PC-2.5; (f) PC-3, and TG curves of different samples

achieved after base and acid pretreatment, respectively, the remained components in the activated carbon were easily degraded and thus increased the mass loss of activated carbon. It was observed that the mass loss of OC, BC and BAC occurred in the range of 300–500 °C, while the mass loss of samples after H_3PO_4 activation with different concentrations occurred in the range of 400–800 °C. This suggested that the structures of samples were changed after H_3PO_4 activation, which became difficult to be oxidized. In order to further study H_3PO_4 -carbon interactions in the activation process, we measured the changes in surface acidic functional groups for samples with different treatments via Boehm titration (Table 4). Compared with OC samples, NaOH or HCl pretreatment improved the amounts of carboxylic, lactonic and carbonyl groups. For PC-0.5 sample, the amounts of carboxylic and phenolic groups significantly increased, while the amounts of lactonic and carbonyl groups decreased compared with BAC samples. With increasing the mass ratio of H_3PO_4 /BAC from 0.5 to 4, the amount of carboxylic and lactonic groups increased, while the amount of phenolic and carbonyl groups gradually decreased. This

indicated that H_3PO_4 affected phenolic and carbonyl groups of activated carbon in the activation process, which matched well with the changes in the FIIR characterization peaks assigned to hydroxyl and carbonyl groups.

XPS was used to analyze the surface chemical characteristics of activated carbon obtained by activation with different concentrations of H_3PO_4 . The C

Table 4 Boehm titration results of samples obtained with different treatments

Samples	The amount of surface species (mmol/L)				Total
	Carboxylic	Lactonic	Phenolic	Carbonyl	
OC	0.17	0.17	0.68	0.43	1.45
BC	0.40	0.23	0.45	0.95	2.03
BAC	0.35	0.90	0.14	0.94	2.33
PC-0.5	2.16	0.14	0.31	0.37	2.98
PC-1	3.15	0.18	0.26	0.36	3.95
PC-2	3.64	0.32	0.21	0.31	4.48
PC-2.5	3.62	0.33	0.20	0.30	4.45
PC-3	3.70	0.34	0.15	0.22	4.41
PC-4	4.72	0.33	0.15	0.18	5.38

indicated that H_3PO_4 affected phenolic and carbonyl groups of activated carbon in the activation process, which matched well with the changes in the FIIR characterization peaks assigned to hydroxyl and carbonyl groups.

XPS was used to analyze the surface chemical characteristics of activated carbon obtained by activation with different concentrations of H_3PO_4 . The C

1s species were deconvoluted into four peaks with binding energies of 284.6, 285.5, 286.5 and 288.9 eV, respectively, corresponding to carbide carbon/graphitic carbon, carbonyl carbon, phenol carbon and carboxylic or lactonic carbon (Figure S4) [41]. The deconvolution of the O 1s species gave four peaks with binding energies of 531.1, 532.2, 533.3 and 534.2 eV, corresponding to carbonyl oxygen, phenol oxygen, lactonic oxygen and carboxylic acid oxygen, respectively (Figure S5) [42]. For C1s peaks, the relative contents of carbonyl and phenol carbon both gradually decreased with increasing H_3PO_4 concentrations (Table S6). The O1s peaks also showed the same trends as that of C1s peaks (Table S7). This supported that H_3PO_4 could interact with carbonyl and phenol groups of activated carbon, which also matched well with Boehm results. The deconvolution of the P_{2p} peak gave two peaks with binding energies of 133.5 and 134.4 eV, corresponding to C–P and C–O–P groups [43], respectively (Figure S6). It could be seen that increasing H_3PO_4 concentrations promoted the growing of C–O–P groups on the surface of activated carbon (Table S8). On the basis of Boehm titration, FTIR and XPS results, it could be speculated that the interaction with H_3PO_4 and the surface phenolic and carbonyl groups may be the reason for the formation of P-containing carbonaceous species. Furthermore, as shown in Fig. 4d, the formation of C–O–P groups would increase the surface area and pore volume of activated carbon when H_3PO_4 /BAC ratio is below 3. With further increasing H_3PO_4 /BAC ratio to 5, the growing of C–O–P groups was significantly promoted; however, the surface area and pore volume of activated carbon decreased. These results further confirmed the formation of C–O–P groups was important, which affected the pore and surface structure of activated carbon. It also indicated that activated carbon-containing P-species can be prepared by adjusting and controlling the textural properties and structures.

Treatment of landfill leachate using prepared activated carbon

The effective treatment of landfill leachate was significantly important for environmental protection. The use of activated carbon for the disposal of landfill leachate attracted worldwide concerns [44, 45]. In order to study the efficiency of prepared activated carbon-containing P-species in the treatment of

landfill leachate, the adsorption results for the treatment of diluted landfill leachate were compared using OC and PC-2.5. A colorless clear liquid was obtained after being treated by PC-2.5 for 1 h, while the color remained yellow after being treated by OC (Figure S7). It was also found that the putrid odor of leachate after being treated by PC-2.5 was obviously weakened compared with that treated by OC. It can be observed from Table 5 that the removal rate of pollutant in leachate was below 1% after being treated by OC, while the removal rate of pollutant in leachate reached 92.4% after being treated by PC-2.5. Foo et al. [26] reported that the removal rate of pollutant from landfill leachate by the treatment of activated carbon was around 16–95%. So an acceptable removal rate was obtained by PC-2.5 in the treatment of landfill leachate in this work. In order to further evaluate the efficiency of the treatment using prepared PC-2.5, several items such as TN, COD, NH_4^+ -N and pH were measured (Table 5). For landfill leachate, the TN was 62 mg/L, while the COD and NH_4^+ -N were, respectively, 1000 mg/L and 18 mg/L. After being treated by OC, the TN of leachate decreased to 25 mg/L, while there were no obvious changes in the COD and NH_4^+ -N. After being treated by PC-2.5, a high removal of TN (84%), COD (82%) and NH_4^+ -N (100%) was obtained. The pH of original landfill leachate was 8.07, and the pH was slightly decreased after different carbons treatments, which met the discharge sewerage standards. These demonstrated the effectiveness of prepared activated carbon-containing P-species by H_3PO_4 activation for the treatment of the landfill leachate.

Discussions

Today, there is still need to develop new technologies that allow us to prepare high-performance carbon materials using agriculture waste residues. The preparation of activated carbon from agriculture waste residues by H_3PO_4 was commonly used; however, the investigation of the structure formation mechanism for the activated carbon in the activation process remained unclear. Li et al. [17] reported that the H_3PO_4 activation of NaOH-treated rice husk residue could obtain activated carbon with maximum surface area of 1016 m²/g. It indicated that H_3PO_4 might act as a catalyst to promote the release of CO_2 and a reagent to enter activated carbon through C–O–

Table 5 Quality of landfill leachate after different treatments

Samples	Removal rate (%) ^b	Items			
		TN (mg/L)	COD(mg/L)	NH ₄ ⁺ -N(mg/L)	pH
Leachate	–	62	1000	18	8.07
Leachate-OC ^a	0.8	25	990	15	7.06
Leachate-PC-2.5 ^a	92.4	10 (84%) ^c	180 (82%) ^d	0 (100%) ^e	5.80

^aThe leachate from original landfill leachate by diluted 12.5 times was, respectively, treated by OC and PC-2.5

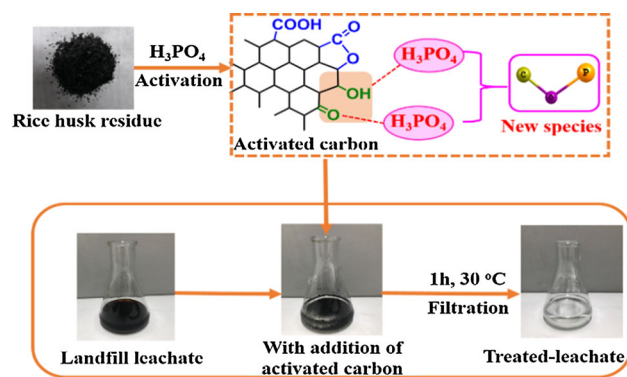
^b The removal rate of pollutant from leachate

^cThe removal rate of TN

^dThe removal rate of COD

^eThe removal rate of NH₄⁺-N

P bonds. However, the performance of H₃PO₄ in the preparation of high-performance activated carbon in this activation process still needs to further investigation. Here, the consequent pretreatments by NaOH and HCl were carried out to remove silica and ash thoroughly, which lead to cracks and pore opening. Without silica and ash effects in activated carbon, H₃PO₄ activation obtained activated carbon-containing P-species with the maximum surface area of 1365 m²/g using agricultural waste residues. Yu et al. [6] reported that the removal of volatile ingredients from carbon in the form of gas could result in the formation of porous structure in the activation process. In addition, the reticulated structure of oxygen and phosphorus conducted to extend the cross-linking polyaromatic, which would promote the development of porosity and higher surface area of activated carbon [46]. H₃PO₄ acting as activation reagent reacted with phenolic and carbonyl groups of activated carbon in the activation process, forming C–O–P species (Scheme 1). As a consequence, the incorporation of C–O–P species by H₃PO₄ activation could result in large amount of pores in the activated carbon, promoting the development of activated carbon porous structure. As shown in Fig. 4d, when the mass ratio of H₃PO₄/BAC was in the range of 2–3, the relative content of C–O–P groups reached around 50%, while the maximum surface area and pore volume, respectively, achieved around 1379 m²/g and 0.67 cm³/g. With further increasing H₃PO₄ concentration, the relative content of C–O–P groups increased, while the surface area and pore volume decreased. The texture properties and structure of activated carbon varied with the relative content of C–O–P groups, which was significantly affected by



Scheme 1 P-containing species were formed in activated carbon and exhibited high efficiency for the treatment of municipal waste leachate.

H₃PO₄ concentrations [Fig. 4d]. Therefore, a suitable content of C–O–P groups obtained with certain H₃PO₄ concentration would benefit for the development of activated carbon porous structure. It seemed that H₃PO₄ acted as the catalyst to adjust and control the textural properties and structure of activated carbon. Furthermore, the P-species formed in the activated carbon exhibited high efficiency for the treatment of municipal waste landfill leachate. The P-species formed in the activated carbon by H₃PO₄ activation showed catalytic effects for the treatment of municipal waste landfill leachate with high efficiency. These findings were helpful to understand the role of H₃PO₄ in the preparation of high-performance activated carbon-containing P-species from agriculture waste.

Conclusion

The present work studied the performance of H_3PO_4 in the preparation of activated carbon-containing P-species from rice husk residues. One possible porous structure formation mechanism of activated carbon-containing P-species by H_3PO_4 activation was proposed. It was found that the NaOH and HCl pretreatments were prerequisite for the increase in the surface area and the development of activated carbons structures. While H_3PO_4 acted as both activation reagent and catalyst in this process. Acting as activation reagent, H_3PO_4 reacted with phenolic and carbonyl groups of activated carbon to form P-containing carbonaceous species, which affected the pore and surface structure of activated carbon. Acting as catalyst, H_3PO_4 activation could adjust and control the textural properties and structures of activated carbon-containing P-species. The cost of prepared activated carbon-containing P-species was low because of waste resources utilization, and the formed P-species showed high catalytic effects to remove over 90% pollutant, 84% TN, 82% COD and 100% $\text{NH}_4^+\text{-N}$ from landfill leachate.

Associated content

Supporting information This material is available free of charge via the Internet at <https://www.springer.com>. BET results, DTG curves, XPS results, FTIR results and the quality of treated landfill leachate results are provided in supporting information.

Acknowledgements

This work is financially supported by the China Postdoctoral Science Foundation (No. 2018M631102), Sichuan Science and Technology Program (No. 2018JY0207), National Natural Science Foundation of China (No. 51478448), the Youth Innovation Promotion Association CAS (No. 2017423), the Deployment Project of Chinese Academy of Science (KFZD-SW-313) and Key Laboratory of Environmental and Applied Microbiology & Environmental Microbiology Key Laboratory of Sichun Province, Chengdu Institute of Biology, Chinese Academy of Sciences (No. KLCAS-2018-5). We would like to thank Yunfei

Tian of Analytical & Testing Center of Sichuan University for XPS experiments.

Authors' contributions

Y.L. carried out the majority of the experiment and wrote the paper. Y.C. and X.S. helped with the analysis of SEM and XRD analysis. Q.C. helped with the treatment of landfill leachate using different carbon samples. D.L. and X.L. supervised the project and revised the paper. All authors have given approval to the final version of the manuscript and contributed to the scientific discussion.

Compliance with ethical standards

Conflict of interest The authors declare that they have no conflict of interest.

Electronic supplementary material: The online version of this article (<https://doi.org/10.1007/s10853-018-03220-x>) contains supplementary material, which is available to authorized users.

References

- [1] Vispute TP, Zhang HY, Sanna A, Xiao R, Huber GW (2010) Renewable chemical commodity feedstocks from integrated catalytic processing of pyrolysis oils. *Science* 330:1222–1227
- [2] Stocker M (2008) Biofuels and biomass-to-liquid fuels in the biorefinery: catalytic conversion of lignocellulosic biomass using porous materials. *Angew Chem Int Ed* 47:9200–9211
- [3] Wong S, Ngadi N, Inuwa IM, Hassan O (2018) Recent advances in applications of activated carbon from biowaste for wastewater treatment: a short review. *J Cleaner Prod* 175:361–375
- [4] Villota EM, Lei H, Qian M et al (2017) Optimizing microwave-assisted pyrolysis of phosphoric acid-activated biomass: impact of concentration on heating rate and carbonization time. *ACS Sustain Chem Eng* 6:1318–1326
- [5] Chingombe P, Saha B, Wakeman RJ (2005) Surface modification and characterisation of a coal-based activated carbon. *Carbon* 43:3132–3143
- [6] Yu X, Wang S, Zhang J (2018) Preparation of high adsorption performance activated carbon by pyrolysis of waste polyester fabric. *J Mater Sci* 53:5458–5466. <https://doi.org/10.1007/s10853-017-1928-2>

- [7] Zhang X, Li Y, Li G, Hu C (2015) Preparation of Fe/activated carbon directly from rice husk pyrolytic carbon and its application in catalytic hydroxylation of phenol. *RSC Adv* 5:4984–4992
- [8] Alvarez J, Lopez G, Amutio M, Bilbao J, Olazar M (2015) Physical activation of rice husk pyrolysis char for the production of high surface area activated carbons. *Ind Eng Chem Res* 54(29):7241–7250
- [9] Fu Y, Shen Y, Zhang Z, Ge X, Chen M (2019) Activated biochars derived from rice husk via one- and two-step KOH-catalyzed pyrolysis for phenol adsorption. *Sci Total Environ* 646:1567–1577
- [10] Liou TH, Wu SJ (2009) Characteristics of microporous/mesoporous carbons prepared from rice husk under base- and acid-treated conditions. *J Hazard Mater* 171:693–703
- [11] Zubrik A, Matik M, Hredzak S et al (2017) Preparation of chemically activated carbon from waste biomass by single-stage and two-stage pyrolysis. *J Clean Prod* 143:643–653
- [12] Jain A, Jayaraman S, Balasubramanian R, Srinivasan MP (2014) Hydrothermal pre-treatment for mesoporous carbon synthesis: enhancement of chemical activation. *J Mater Chem A* 2:520–528
- [13] Kula I, Ugurlu M, Karaoglu H, Celik A (2008) Adsorption of Cd(II) ions from aqueous solutions using activated carbon prepared from olive stone by ZnCl₂ activation. *Bioresour Technol* 99:492–501
- [14] Namane A, Mekarzia A, Benrachedi K, Belhaneche-Bensemra N, Hellal A (2005) Determination of the adsorption capacity of activated carbon made from coffee grounds by chemical activation with ZnCl₂ and H₃PO₄. *J Hazard Mater* 119:189–194
- [15] Song X, Zhang Y, Chang C (2012) Novel method for preparing activated carbons with high specific surface area from rice husk. *Ind Eng Chem Res* 51:15075–15081
- [16] Azmi NB, Bashir MJK, Sethupathi S, Wei LJ, Aun NC (2015) Stabilized landfill leachate treatment by sugarcane bagasse derived activated carbon for removal of color, COD and NH₃-N—optimization of preparation conditions by RSM. *J Environ Chem Eng* 3:1287–1294
- [17] Li Y, Zhang X, Yang R, Li G, Hu C (2015) The role of H₃PO₄ in the preparation of activated carbon from NaOH-treated rice husk residue. *RSC Adv* 5:32626–32636
- [18] Fu Y, Zhang N, Shen Y, Ge X, Chen M (2018) Micro-mesoporous carbons from original and pelletized rice husk via onestep catalytic pyrolysis. *Bioresour Technol* 269:67–73
- [19] Liu X, He C, Yu X et al (2018) Net-like porous activated carbon materials from shrimp shell by solution-processed carbonization and H₃PO₄ activation for methylene blue adsorption. *Powder Technol* 326:181–189
- [20] Li Y, Zhang X, Yang R, Li G, Hu C (2016) Removal of dyes from aqueous solutions using activated carbon prepared from rice husk residue. *Water Sci Technol* 73:1122–1128
- [21] Khan EA, Shahjahan Khan TA (2018) Adsorption of methylene red on activated carbon derived from custard apple (*Annona squamosa*) fruit shell: equilibrium isotherm and kinetic studies. *J Mol Liq* 249:1195–1211
- [22] Danish M, Ahmad T, Nadhari WNAW et al (2018) Optimization of banana trunk-activated carbon production for methylene blue-contaminated water treatment. *Appl Water Sci* 8:1–11
- [23] Ahmad AA, Hameed BH (2010) Effect of preparation conditions of activated carbon from bamboo waste for real textile wastewater. *J Hazard Mater* 173:487–493
- [24] Kamaruddin MA, Yusoff MS, Ahmad MA (2011) Optimization of durian peel based activated carbon preparation conditions for ammoniacal nitrogen removal from semi-aerobic landfill leachate. *J Sci Ind Res* 70:554–560
- [25] Puziy AM, Poddubnaya OI, Socha RP, Gurgul J, Wisniewski M (2008) XPS and NMR studies of phosphoric acid activated carbons. *Carbon* 46:2113–2123
- [26] Foo KY, Hameed BH (2009) An overview of landfill leachate treatment via activated carbon adsorption process. *J Hazard Mater* 171:54–60
- [27] Shen YF (2017) Rice husk silica derived nanomaterials for sustainable applications. *Renew Sust Energ Rev* 80:453–466
- [28] Liu Y, Guo Y, Gao W, Wang Z, Ma Y, Wang Z (2012) Simultaneous preparation of silica and activated carbon from rice husk ash. *J Clean Prod* 32:204–209
- [29] Liu H, Li G, Hu C (2013) Selective ring C–H bonds activation of toluene over Fe/activated carbon catalyst. *J Mol Catal A: Chem* 377:143–153
- [30] Boehm HP, Diehl E, Heck W, Sappok R (1964) Surface oxides of carbon. *Angew Chem Int Ed* 3:669–677
- [31] Gilcreas FW (1985) Standard methods for the examination of water and waste water. *Am J Public Health Nations Health* 56:387–388
- [32] Pradhana BK, Sandleac NK (1999) Effect of different oxidizing agent treatments on the surface properties of activated carbons. *Carbon* 37:1323–1332
- [33] Tseng HH, Wey MY, Fu CH (2003) Carbon materials as catalyst supports for SO₂ oxidation: catalytic activity of CuO–AC. *Carbon* 41:139–149
- [34] Chen Y, Zhai SR, Liu N, Song Y, An QD, Song XW (2013) Dye removal of activated carbons prepared from NaOH-pretreated rice husks by low-temperature solution-processed carbonization and H₃PO₄ activation. *Bioresour Technol* 144:401–409
- [35] Han S, Zhao F, Sun J, Wang B, Wei R, Yan S (2013) Removal of *p*-nitrophenol from aqueous solution by

- magnetically modified activated carbon. *J Magn Magn Mater* 341:133–137
- [36] Cazetta AL, Pezoti O, Bedin KC et al (2016) Magnetic activated carbon derived from biomass waste by concurrent synthesis: efficient adsorbent for toxic dyes. *ACS Sustain Chem Eng* 4:1058–1068
- [37] Brunauer S, Deming LS, Deming WE, Teller E (1940) On a theory of the van der Waals adsorption of gases. *J Am Chem Soc* 62:1723–1732
- [38] Timur S, Kantarli IC, Ikizoglu E, Yanik J (2006) Preparation of activated carbons from *Oreganum* stalks by chemical activation. *Energy Fuels* 20:2636–2641
- [39] Puziy AM, Poddubnaya OI, Martínez-Alonso A, Suárez-García F, Tascón JMD (2002) Synthetic carbons activated with phosphoric acid: I. Surface chemistry and ion binding properties. *Carbon* 40:1493–1505
- [40] Liou TH (2010) Development of mesoporous structure and high adsorption capacity of biomass-based activated carbon by phosphoric acid and zinc chloride activation. *Chem Eng J* 158:129–142
- [41] Ye J, Liu JG, Zhou Y, Zou Z, Gu J, Yu T (2009) High catalytic performance and stability of Pt/C using acetic acid functionalized carbon. *J Power Sour* 194:683–689
- [42] Zhong Y, Li G, Zhu L, Yan Y, Wu G, Hu C (2007) Low temperature hydroxylation of benzene to phenol by hydrogen peroxide over Fe/activated carbon catalyst. *J Mol Catal A: Chem* 272:169–173
- [43] Wu X, Radovic LR (2006) Inhibition of catalytic oxidation of carbon/carbon composites by phosphorus. *Carbon* 44:141–151
- [44] Zhang Y, Pan K, Zhong Q (2013) Characteristics of activated carbon and carbon nanotubes as adsorbents to remove annatto (Norbixin) in cheese whey. *J Agric Food Chem* 61:9230–9240
- [45] Li W, Zhang L, Peng J, Li N, Zhu XY (2008) Preparation of high surface area activated carbons from tobacco stems with K_2CO_3 activation using microwave radiation. *Indus Crops Prod* 27:341–347
- [46] Kan Y, Yue Q, Li D, Wu Y, Gao B (2017) Preparation and characterization of activated carbons from waste tea by H_3PO_4 activation in different atmospheres for oxytetracycline removal. *J Taiwan Inst Chem Eng* 71:494–500